

Available online at [www.sciencedirect.com](http://www.sciencedirect.com)**ScienceDirect**

Procedia Engineering 74 (2014) 47 – 52

**Procedia  
Engineering**[www.elsevier.com/locate/procedia](http://www.elsevier.com/locate/procedia)

XVII International Colloquium on Mechanical Fatigue of Metals (ICMFM17)

## Effects of cyclic pre-straining on mechanical properties of an austenitic microalloyed high-Mn twinning-induced plasticity steel

A.S. Hamada<sup>a,d</sup>, A. Järvenpää<sup>b</sup>, M. Honkanen<sup>c</sup>, M. Jaskari<sup>b</sup>, D.A. Porter<sup>a</sup>,  
L.P. Karjalainen<sup>a,\*</sup>

<sup>a</sup> Centre for Advanced Steels Research, University of Oulu, P.O. Box 4200, FI-90014 Oulu, Finland<sup>b</sup> Oulu Southern Institute, University of Oulu, Pajatie 5, FI-85500 Nivala, Finland<sup>c</sup> Department of Materials Science, Tampere University of Technology, P.O. Box 589, FI-33101 Tampere, Finland<sup>d</sup> Department of Metallurgical and Materials Engineering, Faculty of Petroleum and Mining Engineering, Suez University, Box 43721, Suez, Egypt

### Abstract

The current work was undertaken for gaining insight into the influence of cyclic pre-straining on monotonic flow of a 0.6C-22Mn-0.03V (in wt-%) TWIP steel. Fully reversed tension-compression strain-controlled cycling at four strain amplitudes until the saturation stage was used for pre-straining. The yield and tensile strength and elongation of these cyclically pre-strained samples were measured and compared to those of the non-pre-strained sample. Dislocation structures of the cyclically pre-strained samples were examined using transmission electron microscopy. Cyclic hardening resulting in a saturation stage around the mid-life took place during cycling, the degree depending on the strain amplitude. Tensile testing of cyclically pre-strained samples showed that the yield strength increased by 28% by pre-straining at the strain amplitude of 0.5% for 250 cycles, while the plastic strain amplitude was only 0.15%, the monotonic yield strength increased by 28%, from 500 to 640 MPa. Pre-straining at the 2% amplitude for 40 cycles even doubled the yield strength. The dislocation structure consisting of dislocation cells with a very low number of mechanical twins was found to be a reason for the pronounced strengthening.

© 2014 Elsevier Ltd. Open access under [CC BY-NC-ND license](https://creativecommons.org/licenses/by-nc-nd/4.0/).

Selection and peer-review under responsibility of the Politecnico di Milano, Dipartimento di Meccanica

**Keywords:** High-Mn TWIP steel ; cyclic straining ; cyclic stability ; mechanical properties ; yield stress ; dislocation structure

\* Corresponding author. Tel.: +358 8 5532140; fax: +358 8 5532165.

E-mail address: [pentti.karjalainen@oulu.fi](mailto:pentti.karjalainen@oulu.fi) (L.P. Karjalainen).

## 1. Introduction

High manganese twinning-induced plasticity (TWIP) steels are currently one of the most attractive materials for structural applications in the automotive industry due to their unique combinations of strength and elongation, as reported in several papers, e.g., [1-3]. Consequently, during the recent years, growing interest has been focused on the potential use of austenitic high-Mn TWIP steels in crash-relevant structures of automobiles due to their high energy-absorbing capacity and excellent formability [4]. Bouaziz *et al.* [5] summarized the fundamental knowledge of the plasticity and deformation mechanisms of TWIP steels related to the stacking fault energy and their influence on the mechanical properties, strain-hardening, fracture, and briefly also on fatigue behavior.

Considerable efforts have been directed towards the fatigue behavior of TWIP steels. In this context, Hamada *et al.* [6-8] investigated the fatigue properties and related fatigue damage mechanisms in various high-Mn TWIP steels bearing Al and Si. They reported that the ratio of fatigue limit/tensile strength is 0.42 - 0.48 that is quite similar as commonly observed for various austenitic stainless steels. Dislocation structures consisting of rough labyrinth or vein-type dislocation structures with planar dislocation arrays were observed by Karjalainen *et al.* [9] during the cyclic straining of a 0.29C-16.4Mn-1.54Al (wt-%) TWIP steel. Niendorf *et al.* [10] studied the fatigue properties of the monotonically pre-strained TWIP steel and found that using pre-straining the fatigue strength at the low-cycle regime can be improved significantly. Moreover, they observed a lower dislocation density in the fatigued 0.6C-22Mn TWIP steel compared to that in a tensile strained one, and the density even decreased during cycling.

Chen *et al.* [11] reviewed the mechanical properties of TWIP steels from several publications. They reported that the highest yield strength (YS) could be reached 572 MPa by grain refining to 2  $\mu\text{m}$ . However, the minimum targeted YS for an anti-intrusion and industry application should be 600–700 MPa [12]. Recently, Saha *et al.* [13] succeeded to create nano-structured austenitic TWIP steel with the grain size of 400 nm and the YS of 702 MPa, applying very high cold rolling reduction of 92% with recrystallization at a low temperature to enhance the nanostructure. Economically, this approach to enhance the YS is not desirable in industry because it may increase the manufacturing costs. To the authors' knowledge, the present TWIP steel has been exposed to continuous development over several years to increase the YS by using microalloying elements such as niobium, vanadium and titanium via precipitation strengthening [14-15].

The current work was aimed to study the YS and flow stress behavior of an austenitic high-Mn TWIP steel by applying cyclic plastic deformation to the steel as an exceptional strengthening method. Samples were cyclically strained to the saturation stage before tensile testing to record the monotonic flow behavior and tensile mechanical properties, which were compared with those of non-pre-strained (as-received) sample. Dislocation structures created by cyclic pre-straining were briefly examined by transmission electron microscopy to reveal the origin of strengthening.

## 2. Experimental

The TWIP-type steel containing 0.6C-22Mn-0.3%V (in wt-%) used in this study was laboratory cast and rolled at ArcelorMittal Metz, France. The material was received as 50% cold rolled strips. Further details concerning the steel, casting and hot and cold rolling and coiling parameters can be found elsewhere [15]. Recrystallization annealing of the cold-rolled strips was performed under argon atmosphere at 800 °C for 180 s to ensure the maximum precipitation of V(C,N), approximately 70% (i.e., 0.14 wt-%) of the available alloying [16].

Fatigue specimens, cut in the rolling direction, were machined from the strips with the gauge length of 15 mm and width of 10 mm in accordance with the standard ASTM E8M. Tension-compression fatigue tests were carried out at room temperature at four total strain amplitudes (0.3, 0.5, 1 and 2%) until the failure or only reaching the saturation stress stage. A triangle waveform with a strain ratio of  $R = -1$  was applied at a frequency of 1 Hz. A miniature extensometer with a gauge length of 3 mm was directly attached to the specimens.

After cyclic straining, these cyclically pre-strained samples were tensile strained to failure at a constant strain rate about  $5 \times 10^{-4} \text{ s}^{-1}$  on a Zwick Z 100 universal tensile testing machine equipped with a high resolution extensometer.

Dislocation structures associated with the cyclic straining of the steel were examined by transmission electron microscopy (TEM). Samples were electropolished using a Tenupol 5 device at -15 °C in a solution of 95 pct CH<sub>3</sub>COOH+5 pct HClO<sub>4</sub> and a voltage of 28 V.

### 3. Results and discussion

Fig. 1 shows the cyclic behavior of the steel as the stress amplitude vs. number of cycles at various total strain amplitudes until failure. Table 1 presents more detailed data obtained from the fatigue tests. It can be seen that the steel exhibits a very slight hardening (about 8% increase in the stress amplitude, Table 1) at small strain amplitudes of 0.3 and 0.5%, whereas the degree of hardening is very prominent at higher strain amplitudes of 1 and 2%, 30 and 45% increase in the stress amplitude, respectively. The saturation stress (the highest stress amplitude) is marked by a symbol on the curves, reached after 250, 900 and 5000 cycles at the strain amplitudes of 1, 0.5 and 0.3%, respectively. These fatigue durations were selected for cyclic pre-straining. At the 2% strain, the stress levels after 20 and 40 cycles were taken for pre-straining because hardening was more or less continuous until failure and the formation of any cracks was wanted to avoid.

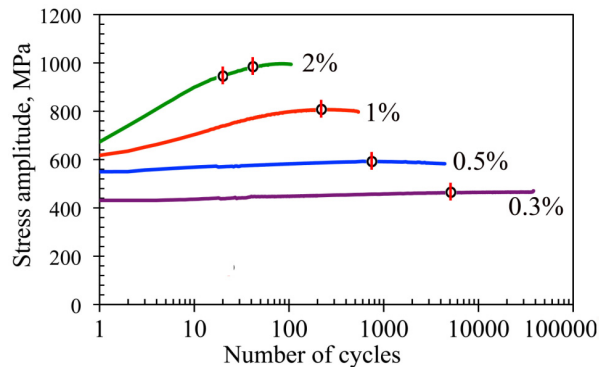


Fig.1. Cyclic behavior of the steel at different strain amplitudes.

Table 1. Cyclic straining data

Sample	Strain amplitude	Life-time	Mid-life	Hysteresis area at mid-life	Stress amplitude at 1st cycle	Stress amplitude at mid-life	Strain hardening at mid-life
	[%]	Cycles	Cycles	MPa	MPa	MPa	%
1	0.3	38100	19050	0.205	330	356	7.9
2	0.3	33400	16700	0.21	336	366	8.9
3	0.3	stop at 5000	5000	0.205	335	360	7.5
AVG	-	35750	17875	0.207	334	361	8.1
1	0.5	4400	2200	2	421	451	7.1
2	0.5	stop at 900	900	1.96	415	461	11.1
AVG	-	4400	-	1.967	419	456	8.8
1	1	683	342	8.91	465	586	26.0
2	1	539	270	10.3	474	618	30.4
3	1	stop at 250	250	9.72	457	598	30.9
AVG	-	611	306	9.7	466	602	29.1
1	2	105	53	38.8	583	858	47.2
2	2	stop at 20	20	41.5	645	904	40.2
3	2	stop at 40	40	47	655	925	45.6
AVG	-	105	-	40.2	614	881	43.7

Deformation structures after cyclic straining were briefly examined. As an example, dislocation structure after cyclic straining of 250 cycles at the 1% strain amplitude is shown in Fig. 2. The dislocation structure was seen to vary from grain to another, but typically it consisted of dislocation cells with dense subboundaries as in Fig. 2a. In one grain, a long, 20 nm thick mechanical twin was observed (Fig. 2b). At lower strain amplitudes, dislocation cells were not so well developed, resembling to the labyrinth structure reported by Karjalainen *et al.* [9] in high-cycle bending fatigue of a 0.29C-16.4Mn-1.54Al steel.

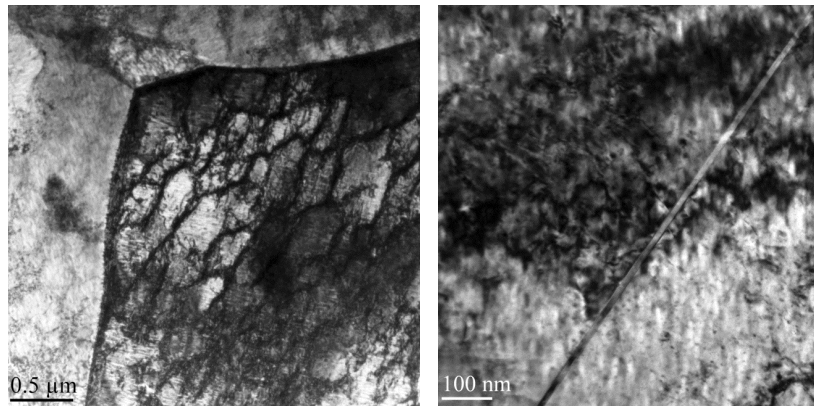


Fig. 2. TEM images of deformation structures after 250 cycles at the 1% strain amplitude revealing well-developed small cells (a) and a single long and very thin mechanical twin (b).

The samples, cyclically pre-strained as mentioned above, were subsequently tensile tested. True stress vs. true strain curves for the cyclically pre-strained specimens are plotted in Fig. 3. A curve for the non-pre-strained sample is also presented for comparison.

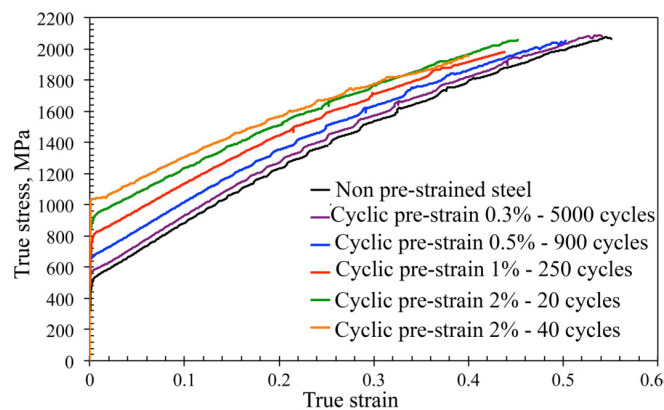


Fig. 3. True stress vs. strain curves for the cyclically pre-strained specimens. Also a flow curve of the non-pre-strained sample is shown for comparison.

YS (i.e., the  $R_{p0.2}$ -proof stress) of the non-pre-strained sample was 500 MPa, tensile strength (TS) 1210 MPa and total elongation 75%. The YS, TS and total elongation values of the cyclically pre-strained samples are listed in Table 2. It can be noticed that YS of the steel has increased from 500 MPa to 560 MPa as pre-strained at the 0.3% strain amplitude for 5000 cycles. Pre-straining at 0.5% for 900 cycles resulted in YS of 640 MPa, hence an increase of 28%. This means that the mean plastic strain amplitudes of 0.13 and 0.15% (predicted from the stress amplitude in Table 1 and the recorded elastic modulus of 170 GPa), which are below the monotonic 0.2% plastic strain used for determining the YS, as imposed several times, results in pronounced strengthening of the steel. Cyclic pre-straining

at the 2% total strain amplitude for 40 cycles even doubled YS. Also some increase in TS occurs with slight decrease in the total elongation, as seen in Fig. 3 and Table 2. The slope of the flow curves, i.e., the strain hardening rate, has slightly decreased due to the pre-straining.

Table 2. Static mechanical properties of the non-pre-strained and cyclically pre-strained samples.

Property	Non pre-strained samples	Cyclically pre-strained samples, SA/ SS				
		0.3/470	0.5/ 601	1/ 785	2/ 943	2/ 1150
YS, MPa	500	560	640	760	900	1000
TS, MPa	1207	1223	1236	1280	1312	1300
A <sub>10</sub> , %	73	70	65	55	57	50

SA: strain amplitude %, SS: saturation cyclic stress MPa, A<sub>10</sub>: total elongation %

In addition, Fig. 3 also reveals serrations in the stress–strain curves which are closely related with the formation of localized Portevin-Le Chatelier (PLC) bands, i.e., dynamic strain ageing. Obviously, the critical strain for the onset of dynamic strain ageing is affected by the cyclic pre-straining, decreasing with increasing strain amplitude used in cycling. This phenomenon has been reported and investigated in high-Mn TWIP steels in tensile testing, e.g., in Refs. [17,18].

If comparing the stress amplitudes at the interrupting stage with the YS (Fig. 1 and Table 2), it can be noticed that the stress amplitude after 5000 cycles at 0.3% is 470 MPa, whereas the YS of this sample in the subsequent tensile test is 560 MPa, i.e., tensile YS is much higher than the stress amplitude. The same is valid for the sample cyclically strained at 0.5% (601 MPa and 640 MPa, respectively). Hence, the cyclic flow has occurred at a lower stress level than the monotonic yield stress. However, contrarily for the cyclically strained samples at 1 and 2%, the opposite is valid (at 1%, 785 MPa and 760 MPa; at 2% for 40 cycles, 1150 MPa and 1300 MPa), the tensile yield stress is much higher than the stress amplitude at the interrupting stage.

If the stress amplitudes at the interrupting stage are plotted as a function of applied total strain (Fig. 4), together with the tensile stress–strain curves of the pre-strained samples, we can notice that the stress amplitudes (i.e., cyclic flow stress) are very close to the monotonic stress at the corresponding strain, i.e., cyclic and monotonic flow stresses correspond closely each other.

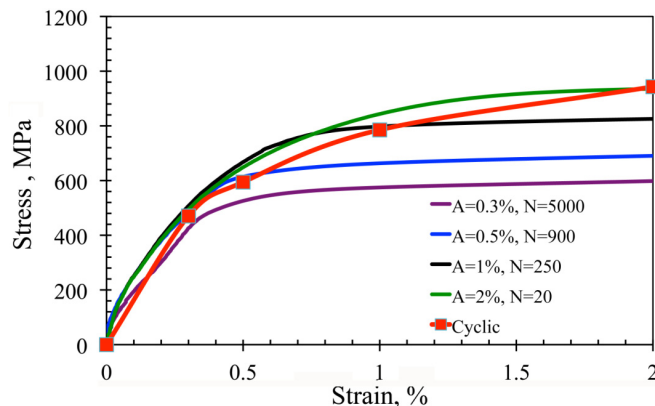


Fig. 4. The cyclic stress–strain curve (red curve with the symbols) in comparison with the monotonic flow stress curves of the pre-strained samples.

It can be concluded that dislocation cells (Fig. 2) and labyrinth structures [9] with few mechanical twins formed in cyclic pre-straining are the reason for the quite pronounced strengthening, seen in the yield strength in particular, and without impaired ductility to any significant amount.

#### 4. Summary

In this work the influence cyclic pre-straining with different strain amplitudes on the flow stress behaviour of high-Mn TWIP steel was studied.

At pre-straining amplitudes 0.3 - 2%, the steel showed cyclic hardening leading to a saturation stage and consequently the monotonic yield strength was increased from 500 MPa (non-pre-strained) even to 1000 MPa (cyclic pre-strained 2% for 40 cycles). The dislocation structure of the cyclic pre-strained samples consisted of dislocation cells along with few mechanical twins resulting in this strengthening without any marked loss of tensile ductility.

#### Acknowledgement

The authors would like to thank Philippe Cugy in ArcelorMittal, Global Research and Development sector, Maizières Automotive Products, France for providing the experimental material.

#### References

- [1] D. Cornette, P. Cugy, A. Hildenbrand, M. Bouzekri, G. Lovato, *Rev. Metall.* 12 (2005) 905–918.
- [2] G. Dini, A. Najafizadeh, R. Ueji, S.M. Monir-Vaghefi, *Mater. Letters* 64 (2010) 15–18.
- [3] R. Ueji, N. Tsuchida, D. Terada, N. Tsuji, Y. Tanaka, A. Takemura, K. Kunishig, *Scripta Mater.* 59 (2008) 963–966.
- [4] B.C. De Cooman, K-G. Chin, J. Kim, in *New Trends and Developments in Automotive System Engineering*, M. Chiaberge (Ed.), 2011, pp. 101–128.
- [5] O. Bouaziz, S. Allain, C.P. Scott, P. Cugy, D. Barbier, *Curr. Opin. Solid State Mater. Sci.* 15 (2011) 141–168.
- [6] A. S. Hamada, L.P. Karjalainen, J. Puustinen, *Mater. Sci. Eng. A* 517 (2009) 68–77.
- [7] A. S. Hamada, L.P. Karjalainen, A. Ferraiuolo, J.G. Sevillano, F. de las Cuevas, G. Pratolongo, M. Reis, *Metall. Mater. Trans. A* 41 (2010) 1102–1108.
- [8] A. S. Hamada, D. Porter, J. Puustinen, L.P. Karjalainen, *Mater. Sci. Forum* 762 (2013) 411–417.
- [9] L.P. Karjalainen, A. Hamada, R.D.K. Misra, D.A. Porter, *Scripta Mater.* 66 (2012) 1034–1039.
- [10] T. Niendorf, C. Lotze, D. Canadinc, A. Frehn, H.J. Maier, *Mater. Sci. Eng. A* 499 (2009) 518–524.
- [11] L. Chen, Y. Zhao and X. Qin, *Acta Metall. Sin. (English Lett.)* 26 (2013) 1–15.
- [12] H-W Yen, M. Huang, C.P. Scott, J-R. Yang, *Scripta Mater.* 66 (2012) 1018–1023.
- [13] R. Saha, R. Ueji, N. Tsuji, *Scripta Mater.* 68 (2013) 813 – 816.
- [14] C. Scott, B. Remy, J-L. Collet, A. Cael, C. Bao, F. Danoix, B. Malard, C. Curfs, *Int. J. Mat. Res* 102 (2011) 538–549.
- [15] C. Scott, P. Cugy, *Proceeding of “International Symposium on Automobile Steel” (ISAS’09)*, China, 2009
- [16] C. Scott, B. Remy, J.L. Collet, A. Cael, C. Bao, F. Danoix, B. Malard, C. Curfs, *Int. J. Mat. Res.* 102 (2011) 538–549.
- [17] S. Lee, Y. Estrin, B.C. De Cooman, *Metall. Mater. Trans. A* 45 (2014) 717–730
- [18] N. Kumar, R.S. Mishra, *Mater. Sci. Eng. A* 580 (2013) 175–183.